

NASA TM-77825

# A Reproduced Copy

OF

NASA-TM-77825 19850015933

NASA TM-77825

Reproduced for NASA

*by the*

**NASA Scientific and Technical Information Facility**

LIBRARY COPY

OCT 10 1985

LANGLEY RESEARCH CENTER  
LIBRARY, NASA  
HAMPTON, VIRGINIA

NASA TECHNICAL MEMORANDUM

NASA TM-77825

CONTRIBUTION TO THE THEORY OF STATIONARY SEPARATION AREAS

G. I. Taganov

Translation of "K teorii statsionarnykh sryvnykh zon," Izvestiya Akademiy Nauk SSSR, Mekhanika Zhidkosti i Gaza, Sept.-Oct. 1968, pp. 3-19.

(NASA-TM-77825) CONTRIBUTION TO THE THEORY  
OF STATIONARY SEPARATION AREAS (National  
Aeronautics and Space Administration) 39 p  
HC 403/AF 801 CSCI 20D

N85-24240

Unclas  
G3/34 21010

NATIONAL AERONAUTICS AND SPACE ADMINISTRATION  
WASHINGTON, D.C. 20546 APRIL 1985



N 85-24244 #

## STANDARD TITLE PAGE

1. Report No. NASA TM 77825	2. Government Accession No.	3. Recipient's Catalog No.	
4. Title and Subtitle CONTRIBUTION TO THE THEORY OF STATIONARY SEPARATION AREAS		5. Report Date APRIL 1985	6. Performing Organization Code
		8. Performing Organization Report No.	
7. Author(s) G. I. Taganov		10. Work Unit No.	
		11. Contract or Grant No. NASA-4006	
9. Performing Organization Name and Address The Corporate Word 1102 Arrott Building Pittsburgh, PA 15222		13. Type of Report and Period Covered Translation	
12. Sponsoring Agency Name and Address NATIONAL AERONAUTICS AND SPACE ADMINISTRATION WASHINGTON, D.C. 20546		14. Sponsoring Agency Code	
15. Supplementary Notes Translation of "K teorii statsionarnykh sryvnykh zon, Izvestiya Akademiya Nauk SSSR, Mekhanika Zhidkosti i Gaza, Sept.-Oct. 1968. pp. 3-19 (A69-12570)			
16. Abstract Analysis aimed at determining the region of existence of steady flows with a closed area of separation for Reynolds numbers at which flow in the region of viscous mixing can be described by the Prandtl's equations. The boundary conditions for the flow in the separation region are selected so as to simplify the flow pattern in this region, making it possible to use the methods of hydrodynamic analysis. A rule for determining stable steady flows with separation areas is formulated which is well suited for analyzing laminar flows and can be applied to turbulent flows in some areas.			
17. Key Words (Selected by Author(s))		18. Distribution Statement unlimited	
19. Security Classif. (of this report) Unclassified	20. Security Classif. (of this page) Unclassified	21. No. of Pages 39	22. Price

---

CONTRIBUTION TO THE THEORY OF STATIONARY SEPARATION AREAS

G. I. Taganov

Experience shows that the pattern of steady flow around /3\* a bluff body with a closed separation area is disrupted at subsonic current velocity at  $R$  numbers from  $10^1$  to  $10^2$  when the flow is laminar in nature. In addition, experience demonstrates that, at supersonic current speed, there is a stable, steady flow pattern if there are laminar stagnation zones adjacent to the body (a stagnation zone behind a reverse ledge on the body's surface, a stagnation zone in front of the smooth ledge on the body's surface, a forward separation area formed by the tip of the centerbody, a stagnation zone formed when there is a descending jump on the body's surface) at high  $R$  numbers on the order of  $10^4$ - $10^6$ .

Thus, experience indicates that, for certain ranges of change in  $M$  and  $R$  numbers under specific boundary conditions, steady solutions to equations for the movement of a viscous liquid exist and are reliable. Outside these ranges and under different boundary conditions, flow around a body with a closed separation area is more (Karman's vortex street at  $M \ll 1$ ) or less (pulsing in close wake behind a body at  $M > 1$ ) clearly definable as steady in nature. There is still no theoretical proof of the existence of stable steady flows with separation areas in these ranges.

Here we attempt to find the region of existence of possible steady flows with a closed separation area in a range of  $R$  numbers such that flow in a viscous mixing area can be described by Prandtl's equations. Limit conditions for flow within the separation area are set so that the flow pattern within the area

---

\*Numbers in the margin indicate pagination in the foreign text.

is considerably simplified and it becomes possible to use hydrodynamic analytical methods.

The first part of this article (points 1-4) studies the field of possible steady flows for an incompressible fluid. It is shown that only under special boundary conditions within the separation area (ideal dissipator) does flow near a smooth slab approach Kirchhoff's flow with quiescent fluid within the zone if  $R$  approaches infinity. The drag coefficient for the "slab + ideal dissipator" system is  $c_x \rightarrow \pi/(\pi+4)$ , i.e. nearly half the value obtained by Kirchhoff for an ideal fluid.

Qualitative study of the field of possible steady flows in plane  $c_x R$  has made it possible to detect the existence of a certain region which has degenerated into a line with an upper limit on the  $R$  number of about  $10^2$ . In this region steady flows possess a particular flow configuration if vortical attachment is not viscous.

The existence of a connection between flow configuration in the region of non-viscous vortical attachment and the reliability of the steady solution is traced in part two (points 6-7), both for individual solutions obtained by methods of the linear theory of hydrodynamic stability and for well-known experimental material obtained over a wide range of  $R$  numbers at sub- and supersonic current velocities. This review makes it possible to formulate a rule for selecting stable steady flows with separation areas and to use it to analyze comparable flows -- both laminar and, in some cases, turbulent.

1. Degenerate flow in a separation zone. We will consider the pattern of a steady flow with closed separation area behind a body past which a current of incompressible fluid flows at  $R$  numbers such as  $R = u_\infty d / \nu$  ( $u_\infty$  is the velocity of the unperturbed current,  $d$  - the transverse dimension of the body), at which the

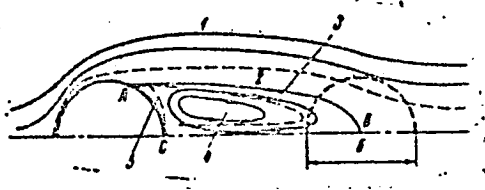


Figure 1

4

thickness of the boundary layer is less than the size of the body (cf. figure 1).

We can identify the following typical lines and areas in the upper half-plane of the flow.

The dividing streamline of the current with fluid segments AB and BC and a segment of the body boundary AC; regions:

1 -- outer potential current; 2 -- outer viscous boundary layer and wake; 3 -- inner viscous mixing layer; 4 -- viscous flow with nearly constant vorticity; 5 -- viscous boundary layer near the rigid boundary of the body with a vorticity opposite in sign; 6 -- attachment. At points on segment AB of the dividing streamline the fluid has a velocity of  $u_p$ , and friction stress  $\tau_p$  is applied clockwise to the fluid moving within the zone. In segment CB, fluid velocity is  $u_0$ ; friction stress equals zero. In segment CA, velocity equals zero, and friction stress applied to the fluid acts counterclockwise.

During steady flow in a separation area, friction forces in segment AB should equal the viscous dissipation of energy within the closed area.

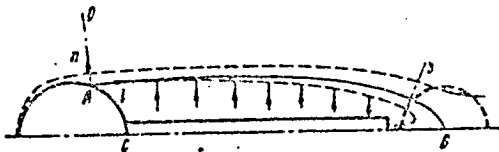
$$\int_{AB} u_p(l) \tau_p(l) dl = \mu \int_F \left[ 2 \left( \frac{\partial v}{\partial x} \right)^2 + 2 \left( \frac{\partial v}{\partial y} \right)^2 + \left( \frac{\partial u}{\partial y} + \frac{\partial v}{\partial x} \right)^2 \right] dF \quad (1.1)$$

Here  $dl$  is an arc element,  $dj$  is an element of the cross section of the area,  $F$  is the area of the cross section limited by line ABCA.

Analysis of values introduced into the integrated expression on the right side of equation (1.1) shows that, if R numbers increase, when the thickness of regions 3 and 5 decreases, velocity gradients in them noticeably exceed the velocity gradient in the core of the flow. Most of the dissipation occurs in these regions, and most energy dissipates in that part of region 3 which is adjacent to section AB of the streamline.

We will try to find conditions under which the pattern of flow within a separation area may be fundamentally simplified. To obtain such a degenerate flow within the separation area, we need to:

- 1) prevent energy dissipation in region 4;
- 2) minimize dissipation in region 5;
- 3) precisely determine energy dissipation  $(E^{(3)})_{AB}$  in that part of region 3 which is adjacent to the streamline AB,
- 4) concentrate dissipation



$$\int_{AB} u_p(l) \tau_p(l) dl = (E^{(3)})_{AB}$$

Figure 2

inadequate to provide a balance in segment CB of region 3, by causing dissipation in an additional element -- an energy dissipator. It is assumed that this additional element, firmly connected to the body, creates a region with high velocity gradients within the separation area, in which dissipation inadequate for balance (4) occurs and that it accepts and transmits to the body the momentum of the backward jet moving toward the body from the attachment region. The shape and dimensions of the dissipator are immaterial to further discussion -- it is considered to be a black box with the ability to reduce the value of Bernoulli constants corresponding to different backward jet streamlines to assigned values.

Figure 2 shows a flow arising in the presence of an ideal dissipator, which dissipates almost all the kinetic energy of the backward jet and assumes the entire momentum of the backward jet gained in segment AB of the dividing streamline.

It is easy to see that, in this case, degenerate flow <sup>/5</sup> (without a circulation core) occurs at constant pressure over the entire region limited by the dividing streamline, except for the attachment region.

A viscous mixing layer develops here at constant pressure and constant outer flow velocity. The tangential component of inner flow velocity on the border of the viscous mixing layer equals zero. Note that there are precise self-similar solutions under conditions close to those considered [1, 2]. We will calculate the residual kinetic energy contained in the backward jet, which must be dissipated in the dissipator, as well as the backward jet momentum which the dissipator must assume.

Let us calculate parameters of the inner part of the viscous mixing layer in cross section S, located at the end of the separation area, but in front of the attachment region in which the flow will be regarded as nonviscous and eddying.<sup>1</sup>

The force of the outer current at the dividing streamline (1.1) is partially dissipated when the quiescent fluid accelerates and is partially used up in creating motion whose kinetic energy in cross section S equals

$$\frac{1}{2}\rho \int_{-\infty}^c n^2(n)dn$$

<sup>1</sup> It is possible to regard flow in the stagnation point region as nonviscous and vortical because of analysis of Navier-Stokes equations in this area. (This has been shown, for example, in a paper by V. V. Sychev at the 8th Symposium on Modern Problems of Fluid and Gas Mechanics. Poland, Tarda, 18-23 September, 1967.)

where  $n$  is the normal to the dividing streamline. This residual kinetic energy should dissipate in the dissipater with an error on the order of  $(v'/u_p)^2$ , where  $v'$  is the velocity of the fluid drawn into the viscous mixing layer from the quiescent fluid in the separation area and the level of dissipation in the section between cross section  $S$  and the dissipater.

Let the non-self-similar viscous mixing layer in cross-section 1 have a certain momentum. It will remain the same in cross-section 2 downstream as well, but will increase in the inner part of the viscous mixing layer in cross-section 2 and decrease by the same amount in the outer part, since the momentum gained by the inner part of the mixing layer at the area of dividing streamline  $l_2-l_1$  will be

$$\Delta V = \int_{l_1}^{l_2} \tau_p(l) dl$$

and the momentum lost by the outer current will be  $\Delta V$ .

If the thickness of the momentum lost at the beginning of the separation area in the outer current is other than zero, then in cross section  $S$ , the momentum gained by the inner part of the current will equal

$$\left[ \rho \int_{-\infty}^0 u^2 dn \right]_1 = \left[ \rho \int_0^{\infty} u(u_k - u) dn \right]_S - \left[ \rho \int_0^{\infty} u(u_k - u) dn \right]_0 \quad (1.2)$$

where  $u_k$  is the velocity at the outer boundary of the mixing layer. If we use the concept of momentum loss thickness  $\delta^{**}$  and introduce the concept of the momentum gain thickness of the inner part of the viscous mixing layer  $\delta_+^{**}$ , determined by the /6 relationship

$$\rho u_k^2 \delta_+^{**} = \rho \int_{-\infty}^0 u^2 dn \quad (1.3)$$



must equal the momentum assumption thickness in cross-section S of the viscous flow:

$$\delta^0 = (\delta_+^{**})_s \quad (1.5)$$

Tractive force T, acting on an ideal dissipator in a viscous degenerate flow<sup>2</sup>, must equal tractive force T<sup>0</sup>, which acts on flow within the constant pressure zone in an ideal fluid model of flow with a backward jet.

In viscous degenerate flow, the ideal dissipator is a flow of impulse, but not a flow of mass. In the ideal fluid potential flow which models the subject viscous flow, sink flow of impulse which equals the power of the sink flow of impulse in an ideal dissipator, is, of course, sink flow of mass.

Pressure drag X<sub>1</sub> acting on a body in viscous degenerate flow must equal pressure drag acting on a body in an ideal fluid model X<sub>1</sub><sup>0</sup>.

The displacing effect a viscous boundary layer developed at a rigid profile has on potential flow is, as we know, determined by the arrangement on the surface of the profile of hypothetical sources, which ensure that potential flow deviates by displacement thickness  $\delta^*$ . Hypothetical sources in an actual viscous flow do not have a current of impulse. In an ideal fluid model, the current of mass from these sources also bears the current of impulse.

In the case considered -- flow with a free boundary -- 17  
current from sources arranged close to the dividing streamline deforms not only exterior potential flow, but also the contour of the constant pressure zone. To obtain from Efros' flow an ideal

---

<sup>2</sup> Here and henceforth, T, X<sub>1</sub>, and X represent total forces valid for two flow regions divided by the plane of symmetry.

fluid model in which viscous effects in the internal and external part of the viscous layer are accounted for in case of degenerate flow in the separation area, sources must be placed close to the free boundary between cross sections 0 and S. These sources must ensure that a random cross section 1 has a mass flow rate of  $\rho u_k (\delta_{+}^{**} + \delta_e^*)$ , where  $\delta_{+}^{**}$  and  $\delta_e^*$  are, respectively, momentum gain thickness and displacement thickness of the outer part of the viscous mixing layer in this cross-section (cf. figure 4.)



Figure 4

Фиг. 4

Indeed, let us extend line L from point N, the dividing streamline of Efros' current (cf. figure 3) in cross section S, to point 0, so that the current of impulse in each section of each layer limited by line L and the free boundary will equal  $\rho u_k^2 (\delta_{+}^{**})_1$  and, correspondingly, the current of mass will equal  $\rho u_k (\delta_{+}^{**})_1$ .

Then for the external flow, line L will become the line of sink flows through which massflows equal to  $\{-\rho u_k (\delta_{+}^{**})_1\}$  can successfully pass. To account for the displacing effect of the external part of the viscous layer, we must arrange along this line both sources which compensate for sinkflow on the line with a flow rate of  $\rho u_k (\delta_{+}^{**})_1$  toward cross section 1, and sources which account for the displacing effect of the external part of the viscous mixing layer with a massflow of  $\rho u_k (\delta_e^*)_1$  toward cross section 1, i.e. with a total massflow toward section 1 equal to  $\rho u_k (\delta_{+}^{**} + \delta_e^*)_1$ .

If in the first approximation we disregard the effect of viscous layer displacement on the configuration of the constant pressure zone, then error in calculating transverse dimension b

of the constant pressure zone will be on the order of  $\delta_e^*/b R_b^{-1/2}$ .

In direct use of Efros' flow in a first approximation of external potential flow near a body with degenerate flow in the separation area, as the preceding indicates, the outer part of the viscous mixing layer is characterized by negative displacement thickness, equal to the momentum gain thickness of the inner flow,  $\delta_+^{**}$ . In other words, an additional error in determining the transverse dimension of the constant pressure zone, on the order of about  $R_b^{-1/2}$ , is permitted.

We will now determine in the first approximation (without regard for actual displacement)  $c_x$  for a "flat slab-ideal dissipator" system as a function of R number, assuming that the initial momentum loss thickness  $(\delta^{**})_0 = 0$  and flow in the viscous mixing layer is self-similar.

In this case, with regard for (1.4), tractive force acting on the ideal dissipator is by definition equal to the total backward jet momentum (since the axial component of the velocity of the fluid from the dissipator equals zero)

$$1/2 T = \rho u_\infty^2 (\delta^{**})_s \quad (1.6)$$

Pressure drag acting on a bluff body,  $X_1$  is about equal to  $X_{1E}$ . Pressure drag acting on a body in Efros' flow is related to backward jet thickness  $\delta_E$  by a ratio obtained from the equation for momentum (cf. [4])

$$\frac{X_{1E}}{2} = \rho u_\infty^2 b_E \left( 1 + \frac{u_\lambda}{u_\infty} \right) \frac{u_\lambda}{u_\infty} \quad (1.7)$$

With regard for tractive force acting on the flow of fluid  $\frac{1}{2} T$  in a backward jet  $1/2 T_E = \rho u_k \delta_E$ , the coefficient for total force of drag acting on the "body + backward jet" system will be

$$c_x = \frac{2X}{\rho u_\infty^2 d} = 4 \frac{\delta_E}{d} \left( \frac{u_k}{u_\infty} \right) \quad (1.8)$$

and the coefficient of pressure drag acting on the body is, from (1.7)

$$c_{x1} = 4 \frac{\delta_E}{d} \left( 1 + \frac{u_k}{u_\infty} \right) \frac{u_k}{u_\infty} \quad (1.9)$$

where  $d$  is the size of the body.

The dimensionless velocity at the current dividing line in a self-similar solution [1, 2] will be

$$U = \frac{u_p}{u_\infty} = 0.567$$

and friction stress on the current dividing line (from [2]) will be

$$\tau_p = 0.2 \sqrt{\mu \rho u_k^3} / l \quad (1.10)$$

where  $l$  is the length of the arc along the dividing streamline from section 0 to the subject section.

The configuration of the flow, and then also for a given  $R$  number, can be determined from (1.5), since the length of cavity  $l_k$  as a function of backward jet thickness is known from the solution of the problem of streamlining a body with backward jet  $\delta_E = f_1(l_k)$ . From the self-similar solution for a viscous mixing layer, we can obtain the function  $(\delta_{+**})_S = (\delta_{**})_S = f_1(l_k)$  for a given  $R$  number.

Integrating (1.10) along the dividing streamline to cross section  $S$ , located distance  $l_k$  from the beginning of the mixing layer, we obtain an equation for the momentum loss thickness of the external part of the viscous mixing layer

$$\rho u_k^2 (\delta_{**})_S = 0.4 \sqrt{\mu \rho u_k^3} l_k \quad (1.11)$$

Substituting the equation for  $\delta_E$  from (1.11) into (1.8), given (1.5) and (1.6), we find

$$c_x = 1.61 \bar{l}_k^{-1/2} \bar{u}_k^{-1/2} R^{-1/2}, \quad l_k = l_k/d, \quad \bar{u}_k = u_k/u_\infty \quad (1.12)$$

Here  $\bar{l}_k$  is the dimensionless length of the cavity in an Efros flow,  $\bar{u}_k$  is the dimensionless velocity at the free boundary.

From (1.8) and (1.9) we have  $c_x = c_{x1}/(1+\bar{u}_k)$ . As we know [4], when  $\bar{l}_k$  approaches infinity, then in an Efros flow near a flat plate  $2\delta_E/d \rightarrow \pi/(\pi+4)$ , and  $c_{x1}$  approaches  $2\pi/(\pi+4)$ , about 0.88, i.e. it tends toward a Kirchoff value for drag coefficient. It is easy to see that (1.5) is satisfied if  $R$  approaches infinity. Consequently, flow in a separation area with an ideal dissipator approaches a Kirchoff flow when  $R$  approaches infinity, and, according to (1.8), when  $u_k$  approaches  $u_\infty$ , the drag coefficient for the "plate + ideal dissipator" system, approaches  $c_x = \pi/(\pi+4)$  or about 0.44, i.e. a value half that obtained by Kirchoff for a separation area with a quiescent fluid at  $\nu=0$ . This is an accurate result, since error from disregarding the effect of displacement approaches zero if the increase in the size of the constant pressure zone is unlimited.

The limitation on the region of existence of stationary 19 flows in terms of  $R$  number imposes the condition  $p_{0p} \geq p_\infty$ , where  $p_{0p}$  is total pressure at the dividing streamline for a nonviscous vortical flow in the attachment region. From Bernoulli equations used in the region of nonviscous attachment to the dividing streamline and to the streamline for the inner potential flow, it follows that

$$\bar{p}_{0p} = \frac{p_{0p} - p_\infty}{1/2 \rho u_\infty^2} = 1 - \bar{u}_k^2 (1 - U^2) \quad (1.13)$$

When  $R$  approaches infinity and  $U=0.587$ ,  $\bar{p}_{0p}=0.345$ . As  $R$  decreases,  $\bar{u}_k$  rises, and for a certain limit  $R$ , value  $R_{lim}$ ,  $\bar{p}_{0p}$  becomes zero. The value  $\bar{u}_k$ , corresponding to this limit  $R$

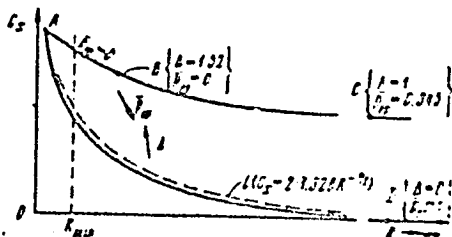


Figure 5

number is found from (1.13) when  $\bar{p}_{0p} = 0$ . For  $U = 0.587$ ,  $\bar{u}_{klim} = 1.23$ , and the corresponding value for pressure resistance in the separation area is

$$\bar{p}_k = \frac{p_k - p_\infty}{\frac{1}{2}\rho U_\infty^2} = 1 - \bar{u}_k^2 = -0.52$$

Let us calculate  $R_{lim}$  and  $c_x$  corresponding to the limit steady flow around a slab with degenerate flow in a separation area. Using results calculated to solve the problem of streamlining a slab according to Efros' system [4], when  $p_k = -0.52$ , we have  $\bar{l}_k$  equal to about 15,  $\bar{u}_k$  equal to about 1.23,  $c_{x1}$  equal to about  $0.88 + 0.52$  and, from (1.8) and (1.9),  $c_x$  equal to about 0.62.

Then, substituting these numerical values into (1.12), we obtain an  $R_{lim}$  of about 120. Thus, in plane  $c_x, R$  (cf. figure 5) all steady flows around a slab with degenerate flow in the separation area lie on curve BC, extending from an  $R_{lim}$  of about  $10^2$  to  $R \rightarrow \infty$ . Along this curve,  $c_x$  for the "slab + ideal dissipator" system varies from about 0.62 to about 0.44.

2. Nondegenerate circulation flow in a separation area. Let us now consider a flow in a separation zone with an imperfect dissipator which permits the existence of circulation motion in a separation area. Batchelor [5] showed that a flat flow of a nonviscous fluid with constant vortex value over the entire circulating flow region, except for a thin layer close to the boundary of the region whose thickness approaches zero when  $R \rightarrow \infty$ .

Let us consider a boundary separating circulation flow with constant vortex from external flow with a zero vortex value. If velocity on the boundary line is less than velocity of the external potential flow at this line, a viscous mixing layer develops if  $\nu$  does not equal zero. Friction stress on the dividing streamline of the viscous mixing layer causes the boundary layer of the circulation flow to accelerate.

Let us place a dissipator across the streamlines of this circulation flow boundary layer which is being accelerated and, consequently, is experiencing a positive increase in Bernoulli constant. Let the dissipator take not all, but only the additional momentum gained by this boundary layer when exposed to friction stresses on the dividing streamline and let it release fluid with the same Bernoulli constant distribution across the streamlines as was in this layer before it accelerate near the dividing streamline. The presence of a dissipator with these properties in the separation area with circulation motion /10 makes it possible to satisfy equations for energy and momentum.

The velocity of the external potential flow  $\bar{u}_k$  and the velocity at the boundary layer of the circulation flow with constant vortex  $\bar{u}_b = u_b/u_\infty$  along the common boundary are related by the equation

$$\Delta = \bar{u}_k^2 - \bar{u}^2 = \text{const} \quad (2.1)$$

resulting from the equality of static pressure in the external and internal flow at each point on the boundary [6]. The constant introduced into (2.1) can be used as an independent

parameter defining flow and, accordingly, dissipator properties.<sup>3</sup>

An ideal fluid model describing the external potential flow near a body with a separation area with circulation flow in it and accounting for all viscous effects is built similar to that in point 1. The dissipator in a viscous flow will be a sink flow of mass; in the ideal fluid model, a sink flow of impulse with something like the power of a sink flow of mass will correspond to it. Strictly speaking, the location of this sink flow should correspond to the location of the dissipator in the separation zone (in this it differs from degenerate flow).

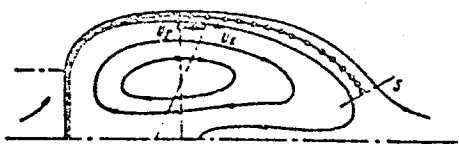


Figure 6

The currents of mass in any radial cross section of circulation flow in an ideal fluid model are identical (cf. figure 6). Calculation of parameters for flow in a viscous mixing layer (defining  $U(l)$ ,  $\delta^{**}(l)$ ,  $\delta_e^*(l)$ ) is complicated because the difference in velocities on the boundaries of the layer, as well as static pressure, varies along the viscous layer.

There are also calculating problems in finding flow in an ideal fluid model, resulting because one region of flow satisfies Laplace's equation, while the other -- the inner -- satisfies

---

<sup>3</sup> If a portion of the friction surface of the body acts as a dissipator, then parameter  $\Delta$  is defined by the condition

valid for a boundary layer periodic in terms of  $l$  at high  $R$  numbers.

Poisson's equation. We can approximately replace flow with constant vortex equivalent to it in terms of current of impulse by M. A. Lavrent'yev's potential ring [7] and seek a solution to the problem in the class of harmonic functions. Numerical calculations are carried out in this approximation.

3. The Region of stationary flow in plane  $c_x R$ . Without data from numerical calculations on flow with circulation motion within a separation area, we will try to qualitatively evaluate the location in plane  $c_x R$  of stationary flows which satisfy various values for parameter  $\Delta$  (cf. figure 5). Steady flows with an ideal dissipator in the separation area for which  $\bar{u}_b = 0$  correspond to points on curve BC. According to calculation, parameter  $\Delta$  varies monotonically along the curve, according to calculation, from  $\Delta_B$  of about 1.52 to  $\Delta_C$  equal to 1. The lower boundary of the region of steady flow with circulation motion in the separation zone in plane  $c_x R$  must be curve AD, which corresponds to a maximally weak dissipator (friction on the back side of the slab). It is easy to show that the drag of a slab streamlined in the separation area corresponding to points on curve AD is on the order of the friction drag in the same slab, past which a current flows at the same R number, but below zero incidence, i.e. curve AD is close to curve L, described by the equation  $c_x = 2(1.328R^{-1/2})$ .

$$[\rho \int_{-\infty}^0 u(x - x_r) dx_r]_b = 0$$

Parameter  $\Delta$  on curve AD cannot become zero when R number is finite, since the finite friction impulse on the back side /11 of the slab which decelerates the circulation flow within the area and the absence in this case ( $\bar{u}_k^2 - \bar{u}_b^2 = 0$ ) of an accelerating impulse from the internal flow at the dividing streamline would violate the equality  $\bar{u}_k^2 - \bar{u}_b^2 = 0$  and create a new circulation flow with a  $\Delta > 0$ . Parameter  $\Delta$  can become zero only if the decelerating friction momentum on the back side of the slab becomes zero, i.e. if  $R \rightarrow \infty$  (point D). If  $R \rightarrow \infty$ ,  $\Delta$ , which describes dissipator efficiency, passes through all values between zero at point D ( $c_x \rightarrow 0$ ) and unity at point C ( $c_x \rightarrow \pi/\pi+4$ ). Keeping this in

mind and relying on the distribution of  $\Delta$  calculated along curve BC, we can expect that the behavior of lines  $\Delta = \text{const}$  in plane  $c_x R$  is close to that presented in figure 5.

We will now determine how the shape of the separation area close to the slab and the flow close to it vary when  $R \rightarrow \infty$  as dissipator efficiency decreases, i.e. during movement from point C toward point D. Point C represents an infinitely long separation area, as indicated above. The unlimited size of the separation area for points located between C and D when  $R \rightarrow \infty$  results from the finite nature of  $c_x$  at these points.

Even an approach to point D along curve AD does not contradict the assertion that a flow corresponding to point D also belongs to a class of flows with unlimited separation area dimensions. The length of the separation area must increase in flow corresponding to points on curve AD if  $R \rightarrow \infty$ ; otherwise the accelerating momentum, applied to the circulation flow at the dividing streamline approaching zero as  $R^{-1/2}(\bar{u}_k^2 - \bar{u}_b^2)\bar{l}_k$ , would decrease more quickly than the impulse of friction on the back side of the slab approaching zero when  $R^{-1/2}$ .

Flows with a vorticity  $\Omega$  of about  $u_\infty/b$ , where  $b$  is the transverse dimension of the area, correspond to all points of segment CD, except degenerate flow in the area corresponding to point C. Since the size of the area increases without limit when  $R \rightarrow \infty$ , flow within the separation zone at a distance on the order of  $d$  from the slab approaches local potential.

Consequently, at the tangential discontinuity separating the separation area, it is not vorticity, but the Bernoulli constant that is disrupted if  $\Delta > 0$ .

The shape of the separation area in plane  $xy$  when the fluid in the separation zone is quiescent, taken from Kirchoff's well-

known solution, is given in figure 7.

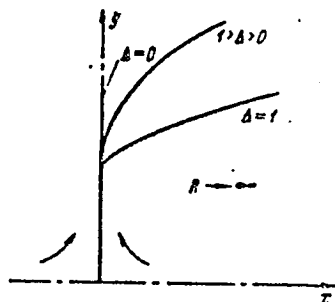


Figure 7

Фиг. 7

If we assume the existence in this contour of a potential flow with  $\Delta > 0$ , then pressure at the stagnation point on the back side of the slab will become greater than  $p_{\infty}$ . It will also increase in the angular region of the subject contour adjacent to the slab. To fulfill the condition of equality of static pressures for both sides of the contour, it must deform -- the curvature of the contour in the angular region must decrease as compared with initial curvature. As parameter  $\Delta$  decreases, the curvature of the contour should diminish (cf. figure 7). We can find the shape of the separation area contour from the solution of the problem of streamlining a slab with two oncoming clean currents for which the difference in Bernoulli constants is set when static pressures are equal and the fluid contour is impenetrable.

Streamlining a slab with two oncoming clean currents with identical Bernoulli constants ( $\Delta=0$ ), which provides a local flow pattern near the slab, a pattern corresponding to point D on plane  $c_x, R$ , is worth discussing.

It is easy to be sure that the conditions of the problem are satisfied by a potential flow whose flow function is

$$\psi = -kxy \quad \left( u = \frac{\partial \psi}{\partial y} = -kx, v = -\frac{\partial \psi}{\partial x} = ky \right) \quad (3.1)$$

Coefficient  $k$  from the condition that velocity is limited at

an infinite (to the scale of dimension  $d$  of the slab) distance from the slab should approach zero, and flow near the slab should become quiescent (cf. figure 8, a).

Thus the limit condition for the flow of a viscous fluid /12 near a slab with a separation zone when  $R \rightarrow \infty$  is in fact, as Batchelor first stated [6], by  $c_x \rightarrow 0$ . However, the flow pattern turned out to be quite different from that assumed. Nonetheless, the resulting flow near the slab satisfies hydrodynamic equations and provides another description of D'Alembert's paradox for flow around a slab: it accounts for the need to form a separation area because of the effect of viscosity, which is usually disregarded (cf. figure 8, b).

Let us turn now to the other end of region ABCD -- to small  $R$  numbers.

Curve AB is the boundary of the region of possible steady flows. Its points represent limit flows for which the equation  $\bar{P}_{0p} = (P_{0p} - P_\infty) / 1/2 \rho u_\infty^2$  in the region of nonviscous vortex attachment becomes zero.

Using calculations of the change in  $\bar{P}_{0p}$  along curve BC, which varies monotonically in  $R$  number from  $(\bar{P}_{0p})_B = 0$  to  $(\bar{P}_{0p})_C = 0.345$ , and taking into account that  $P_{0p}$  approaches 1 when parameter approaches zero, we can construct the preferred pattern for locating lines  $\bar{P}_{0p} = \text{const}$  in the region ABCD (cf. figure 5).

Of course, when analyzing flows in the region of low  $R$  numbers, we must keep in mind that the original assumption that flow in a viscous mixing layer can be described by Prandtl's equation and that circulation flow within an area can be described by Euler's equations are invalidated for a certain value  $R_{\min}$ , and if  $R < R_{\min}$ , flow is described by Navier-Stokes equations.

4. Unique features of flow in the region of nonviscous vortical attachment when  $\bar{p}_{0p}=0$ . Figure 9 presents possible alternatives for pressure distribution

$$\bar{p} = \frac{p - p_{\infty}}{1/2 \rho u_{\infty}^2}$$

along the plane of flow symmetry for nonviscous attachment of vortical currents in a separation area behind a body, which correspond to various points in region ABCD and its boundaries. At the maxima for these curves, we have  $\bar{p} = \bar{p}_{0p}$ , and the position of the maximum along the x-axis determines the position of the stagnation point behind the separation area along the y-axis.

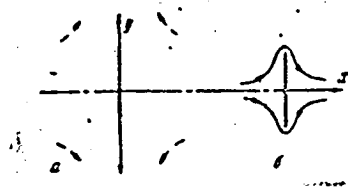


Figure 8

If, for flows 1 and 2, for which  $\bar{p}_{0o} > 0$ , the stagnation point lies farthest from the separation zone, then for flow 3, for which  $\bar{p}_{0p} = 0$ , three types of pressure distribution curves along the plane of symmetry are conceivable: 3a -- pressure maximum lies within the flow, but there must be at least one pressure minimum downstream of it; 3b -- pressure maximum is achieved within the flow, but downstream of it, pressure is constant and equals pressure at an infinite distance; 3c -- the stagnation point lies an infinite distance from the stagnation zone. Using A. A. Nikol'skiy's theorem [8] on the monotonic nature of the change in the slope of the velocity vector during movement of a gas along the equal pressure line in a flat subsonic vortical flow, we can show that flow conditions described by curves 3a and 3b are impossible in the case we are discussing.

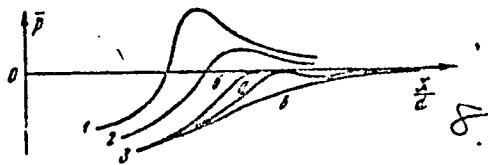


Figure 9

If we extend the constant pressure line near the assumed minimum pressure lying downstream of the pressure maximum corresponding to condition 3a, then the ends of this constant pressure curve lying on the plane of symmetry will be /13 represented by identical velocity vector slope values, and this will contradict Nikol'skiy's theorem, which requires that velocity vector slope increase if the length of the equal pressure line is finite.

If we extend the constant pressure line from the point corresponding to the assumed pressure maximum in 3b, then it goes into infinity, where the velocity vector slope is also equal to the velocity vector slope at the plane of symmetry, i.e. we will arrive at the contradiction already discussed.

Consequently, when  $\bar{p}_{0p} = 0$ , the nonviscous vortical flow in the attachment region has a configuration (cf. figure 10) such that the stagnation point does not lie in the finite region of the flow. In this flow configuration, the dividing streamline (denoted in figure 10 by the thick line) limits the thin tongue of the nonviscous backflow extending downstream to infinity.



Figure 10

Thus, points on boundary AB of region ABCD (cf. figure 5) represent steady stalled flows whose stagnation point does not lie in the finite region of the flow when attachment is

nonviscous and vortical. In other words, these flows have a configuration in attachment regions significantly different from that of a flow with a stagnation point in the finite attachment region, which is typical of flows filling the entire region ABCD.

The existence of a connection between the configuration of a flow in the nonviscous attachment region and the stability of a steady flow with a separation area is traced in points 6 and 7.

5. Steady flows with separations areas when  $M > 1$ . When  $M > 1$ , only part of the total loss in momentum caused by base drag lies in the vortex wake. Most of the momentum loss is caused by the wave drag of the fluid contour of separation area  $X_2$  and lies in waves moving downstream from the separation area boundary.

Base drag of a flat body of finite length will be

$$\frac{1}{2}X = \rho u_{\infty}^2 \delta_{\infty}^{**} + \frac{1}{2}X_2$$

The coefficient of bottom drag related to the velocity head of an unperturbed flow and to the finite dimension  $d$  of the body in the base shear region will then be

$$c_x = 2\delta_{\infty}^{**} / d + c_{x2}$$

If  $(\delta_{\infty}^{**})_0 = 0$  and flow in wake behind the shear region is considered nonviscous and vortical, then wave drag in the fluid contour of the separation zone can be written as

$$c_{x2} = c_{x2f} (1 - 2\delta_{\infty}^{**} / d)$$

Here  $c_{x2f}$  is the coefficient for the wave drag of the fluid contour of the separation area related to the height of the fluid ledge  $d - 2\delta_{\infty}^{**}$ .

Clearly, the wave portion of base drag depends on the shape of the separation zone's fluid contour and wave displacement thickness. The development of wave drag, which is a function of the separation zone's fluid contour, and separation zone contour

as a function of circulation flow intensity within the area make it much more complicated to find possible steady flows in plane  $c_x R$  over a wide range of changes in dissipator properties. However, for degenerate flow within the area, i.e. if an ideal dissipator is present, the problem is considerably simpler and possible constant-property flows can be found. We will limit ourselves here to discussing the case of a degenerate flow within the area when  $R \rightarrow \infty$  and  $\delta_{**} = 0$ . The self-similar precise solution for a laminar layer on the dividing boundary mixing a jet of compressed gas with a quiescent gas when  $\mu p = \text{const}$  from [2, 14] gives us

$$U = \frac{u_p/a_0}{u_h/c_0} = \frac{\lambda_p}{\lambda_h} \approx 0.557 \quad (5.1)$$

Total pressure on the dividing streamling in the non-/14  
viscous attachment region is calculated from

$$\frac{p_{0p}}{p_{\infty}} = \frac{p(\lambda_h)}{p(\lambda_p)p(\lambda_{\infty})}, \quad p(\lambda) = \left[ 1 - \frac{\gamma-1}{\gamma+1} \lambda^2 \right]^{\frac{\gamma}{\gamma-1}}, \quad \gamma = \frac{c_p}{c_v} \quad (5.2)$$

Static pressure within a separation area which has a straight boundary is constant over the entire area;  $\delta_{**}/d \rightarrow 0$  and  $\delta_{**}/d \rightarrow 0$  when  $R \rightarrow \infty$ , while  $c_x \rightarrow c_{x2f}$ . Static pressure in the area, which determines base drag is in this case obtained from the ratio

$$\frac{p_k}{p_{\infty}} = \frac{p(\lambda_k)}{p(\lambda_{\infty})} \quad (5.3)$$

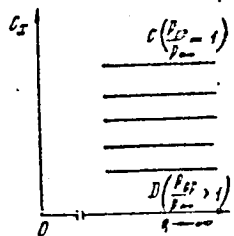


Figure 11

From (5.1)-(5.3) for a given  $\lambda_{\infty}$ , we can calculate  $p_k/p_{\infty}$  which corresponds to possible steady flows when  $R \rightarrow \infty$  in plane  $c_x R$  (cf.

figure 11). Point D represents  $p_{0p}/p_\infty > 1$ , point C corresponds to the limit flow with a separation area  $p_{0p}/p_\infty = 1$  and limit values  $(p_k/p_\infty)_{lim}$  with  $c_{xlim}$ .

We can show that flow configuration in a nonviscous vortical attachment region with infinitely long return flow tongue corresponds only to limit flow  $p_{0p}/p_\infty = 1$ , just as to limit flow  $\bar{p}_{0p} = 0$  when  $M \rightarrow 0$ . All remaining steady flows with  $p_{0p}/p_\infty > 1$  contain a stagnation point in the finite region of the nonviscous vortical attachment region.

Using the theorem of monotonic change in velocity vector slope along a constant pressure line located in the subsonic region of a flow adjacent to the plane of symmetry, i.e. assuming that we can always select a constant pressure line close enough to the proposed minimum pressure that this line is within the subsonic region of the flow, we will establish that such a pressure minimum is impossible, i.e. that condition 3a (cf. figure 9) is impossible.

The hypothesis that condition 3b can exist implies that pressure must be constant over the entire subsonic region of a flow located downstream of a constant pressure line extended from the point of the assumed pressure maximum. But this in turn requires that both pressure in the supersonic region and velocity vector slope be constant. During flow around a flat

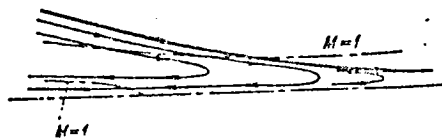


Figure 12

body of infinite length with curved shock waves upstream, this requirement cannot generally be fulfilled. The configuration of flow in a nonviscous vortical attachment region, corresponding to limit flow with  $p_{0p}/p_\infty = 1$ , is shown in figure 12.

6. On the existence of a relationship between configuration of flow in a nonviscous vortical attachment region and flow stability. As we know, study of the stability of a given steady flow in terms of low velocity and pressure perturbations depending on time and coordinates presents a difficult hydrodynamic problem which, within the framework of the linear theory, can be solved only for individual simple configurations of viscous steady flows. Study of the stability of viscous steady flow with a separation area of complex configuration also presents problems which are yet to be overcome. However, study of the hydrodynamic stability of nonviscous steady fluid flows involves fewer mathematical difficulties. Therefore, we do have some results, obtained with the theory of hydrodynamic stability for several nonviscous flows of incompressible fluids of complex configuration with partially free and partially rigid boundaries which contain regions of jet attachment or connection [9; 10].

The potential flows of incompressible fluids with both /15 free ( $p = \text{const}$ ,  $\rho' = 0$ , where  $p$  is static pressure at the boundary, and  $\rho$  is the density of the medium adjacent to the subject flow) and straight rigid boundaries which are studied in these references include:

a) flows which are stable or neutral to minor perturbations over the entire range of change in wave number of the imposed perturbed flow, except one isolated wave number, for which the flow is unstable. A typical feature of the configuration of these flows is the lack of a stagnation point in the finite region of the main flow;

b) flow which is stable or neutral to minor perturbations. The stagnation point of this flow lies on a rigid boundary of finite length;

c) flow which is unstable for minor perturbations over a wide range of wave number changes and has a stagnation point within

the finite region of the main flow;

d) flow which is unstable for minor perturbations over a wide range of wave number changes and has a stagnation point on a rigid boundary of infinite length in the finite region of the main flow.

Thus, for the potential flows of incompressible fluids with partially free and partially rigid boundaries reviewed in these articles, instability occurs if the stagnation point lies in the finite region of the main flow and not on a rigid boundary of finite length. On the other hand, flows with a stagnation point outside the finite region of the main flow are virtually stable.

This result of the linear theory of hydrodynamic stability is important for analyzing the causes of instability of flows with separation areas, which has been observed in experiments with specific ranges of  $R$  and  $M$  numbers for specific boundary conditions within the separation area. Since nonviscous flow in the stream attachment region beyond the separation area which we have discussed is close in configuration to that class of flows with partially free and partially rigid boundaries studied in the theory of hydrodynamic stability, the conditions given above which determine the stability or instability of potential flows must be considered when analyzing the flow we are considering.

The assumed position of the stagnation point in the nonviscous attachment region behind the separation area, a finite distance from the separation area in the plane of symmetry (or on the rigid boundary of infinite length when attachment is to the flat surface of an extended body beyond the nonsymmetric separation area) creates a situation in which potential analogs of the subject flow are unstable. On the other hand, we must bear in mind that potential analogs of the subject flow are stable, if nonviscous vortical flow in the attachment region beyond the separation area does not contain the stagnation point

in the finite region, and the configuration of the flow with an infinitely long backflow tongue develops.

If we use the hypothesis that the instability of a nonviscous flow in an attachment region (caused, as shown by the examples of flows studied by the linear theory of hydrodynamic stability, by the configuration of flows in the attachment region) is the main reason for the instability of the entire viscous flow with separation area, then the rule for determining stable steady flows with separation areas will be that velocity in the finite region of the nonviscous vortical attachment not be zero.

The validity of this hypothesis can be determined (at least at present) only by using the determination rule to compare the ranges of existence of stable stalled flows with the ranges of existence of stable steady flows observed in experiments over a wide range of changes in  $R$  and  $M$  numbers. Let us make this comparison.

1. Incompressible fluid. According to calculations in points 1-4 for flow around a flat slab with a separation area, the region of steady flows which satisfy the selection rule is limited by an  $R$  number of about  $1.2 \times 10^2$ . This  $R$  number corresponds to a strong dissipator in the separation area. If the dissipator's efficiency decreases, the  $R$  number at which a steady flow with separation area is disrupted diminishes.

We know that experimental  $R$  numbers at which a steady flow is disrupted (called critical  $R_*$  number in literature), measured in wind or hydrodynamic tunnels are a function of the ratio of transverse dimension  $d$  of a cylindrical body to height  $H$  of the cross section of the working part of the tunnel.

Thus, according to [11], steady flow around a round-section cylinder with a separation area is preserved up to  $R_*=30$  when  $d/H=0.025$  and to  $R_*=62$  when  $d/H=0.10$ . Therefore, calculated  $R_*$

values determined for an unrestricted current must be compared with experimental data obtained at small  $d/H$  values.<sup>4</sup> With regard for this circumstance, it follows from experimental data for flow around a round-section cylinder with a weak dissipator (friction on the back side of the cylinder) that  $R_*$  is about 30. If a dividing slab whose length is comparable to the length of the separation area is placed within an area with a plane of flow symmetry, steady flow is extended to higher  $R$  numbers.

In this way Acrivos and his associates [12] successfully increased  $R_*$  several times to about 170 when  $d/H=0.05$  (recent experiments by Acrivos<sup>5</sup> with small  $d/H$  values give an  $R_*$  of about 100). Calculation of the force of friction applied to a dividing slab on the backward jet side shows that tractive force exceeds half the momentum of a backward jet whose parameters were calculated for a degenerate flow.

A dividing slab is thus a strong dissipator, and the  $R_*$  of about 100 obtained by Acrivos' experiments is comparable to the predicted  $R_*$  of about 120 for flow around a slab with a maximally strong dissipator. Base drag coefficients when  $R$  is approximately equal to  $R_*$  are also comparable: calculated  $\overline{P}_k = -0.52$ , experiment  $\overline{P}_k = -0.45$ .

Of course, when making this comparison we must keep in mind that the bodies differ in shape. However, the correlation obtained is quite promising for a first attempt, because, as far as we know, it has never been possible to obtain theoretical evaluations of the  $R_*$  numbers at which Karman's vortex street occurs since this flow shape was first observed.

---

<sup>4</sup> Calculated  $R_*$  values for flow around a body located between parallel walls increase as  $d/H$  increases.

<sup>5</sup> This comes to the author from V. V. Sychev.

The configuration of cavitation flows is close to that of the subject stalled flows. The fact that cavitation flows with closed cavities are steady flows at positive cavitation numbers  $Q = (p_\infty - p_k) / \frac{1}{2} \rho u_\infty^2$  is now commonly known [13]. However, using the determination rule for cavitation flows makes it possible to predict the existence of a broad region of stable steady cavitation flows when gas is released into a cavity and at negative cavitation numbers. In this case, given a nonviscous connection with various Bernoulli constants, there is generally no stagnation point beyond the cavity, or, given a negative cavitation number,  $p_0 > p_\infty$  on all streamlines coming from the cavity.

2. Supersonic velocities. Point 5 showed that, when  $R \rightarrow \infty$  and there is a strong dissipator in the separation area, there are many possible steady flows which satisfy equations for gas dynamics of a viscous fluid, for which there are various corresponding base pressure values  $p_k / p_\infty$ . However, only one, corresponding to point C (cf. figure 11) can be considered a stable steady flow, since the configuration of the flow in the nonviscous vortical attachment region which corresponds to point C satisfies the selection rule.

As we know, Chapman and associates [14], in careful /17 experiments on the stalled flow behind the reverse ledge on the surface of a body at  $1.3 < M < 2.0$  for  $R$  numbers from  $0.6 \times 10^4$  to  $1.4 \times 10^6$ , observed the existence of laminar flow within a separation area at these high  $R$  numbers, in which base pressure varies as a function of  $M$  number in quite close quantitative correspondence with values calculated for point C ( $p_{0p} / p_\infty = 1$ ). Just as in Acrivos's experiments, the surface of the body behind the ledge adjacent to the separation area is a strong dissipator in Chapman's experiment, which justifies comparing experimental

data with calculations for a maximally strong dissipator.<sup>6</sup> In summary, we can conclude that the hypothesis that configuration of flow in a nonviscous vortical attachment region has a decisive effect on the stability of steady flows with separation areas is confirmed by existing experimental data on laminar separation areas over a wide range of changes in R and M numbers. This makes it possible to apply this hypothesis in theoretical analysis of stalled flows.

7. On the use of the selection rule in studying stalled flows.

1. Turbulent flow in a separation zone. As we know, the openness of the system of Reynold's equations which describe vortical motion does not permit theoretical study of even the simplest instances of turbulent flows without using empirical quantitative data. In addition, use of empirical data makes it possible to calculate parameters for averaged turbulent flow for simple flow configurations (a wall turbulent boundary layer, a turbulent mixing layer on the boundary of a jet flowing out of an immersed space, the main portion of a turbulent jet).

---

<sup>6</sup> Note that Chapman's use of the correlation between  $p_{0p}/p_{\infty}$  and bottom pressure, observed in experiments at supersonic velocities (when flow was steady) and used in the Chapman-Korst calculating procedure (this procedure will be discussed in more detail later) for interpreting Roshko's experimental data [15] on base pressure behind a round-section cylinder with a dividing slab at an R of about  $10^4$ , is, in the light of what has been presented above, unjustified, since, in Roshko's experiments, flow behind a round-section cylinder with a dividing slab was periodic (without constant properties) in nature at these R numbers.

We might expect that results satisfactory from an engineering standpoint can be obtained by calculation and by study of complex configurations of turbulent flow if they contain components which are simple configurations of turbulent flow studied in detail in "pure" form.

If these components cannot be identified in pure form in a turbulent flow of a complex configuration, then quantitative empirical data for the subject complex configuration of turbulent flow must be accumulated before calculation. Turbulent flow in a separation area has a complex configuration, but there is still little quantitative empirical data for it. Therefore, we will limit ourselves to discussing degenerate flow in which a turbulent mixing layer separates external flow from quiescent fluid within a separation area with constant pressure, since, in considering turbulent flow with a circulation core, we already cannot ignore turbulent friction stresses and energy dissipation within the core, which cannot as yet be calculated because of lack of quantitative empirical data for a random circulation core contour shape.

For a completely turbulent flow in a separation area,  $R$  number determines only the nature of flow in the boundary layer on the surface of the body up to the flow separation point and the thickness of the boundary layer at the beginning of the turbulent mixing layer, which in turn define the position of flow separation on the body's surface and indirectly affect  $U$  and  $\tau_p$  values. These same equations, which describe flow in a turbulent mixing layer, do not contain molecular viscosity  $\nu$  and, consequently,  $R$  number.

Let us consider flow around a slab at a  $(\delta^{**})_0$  which does not equal zero and an  $M \ll 1$  with degenerate flow within the separation area from a maximally strong dissipator.

The decisive parameters of a turbulent mixing layer ( $U$ ,  $\tau_p$ ) are a function of  $(\delta^{**})$  and empirical constant  $\sigma$  (proportional to the angle of expansion of the turbulent mixing layer). By making judgments similar to those in point 1 to

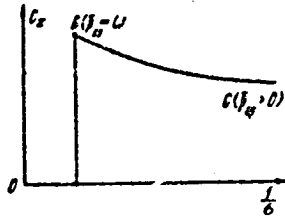


Figure 13

plotting  $c_x = f(R)$  for a laminar mixing layer, we can, for a given  $(\delta^{**})$ , find possible steady flows for a turbulent degenerate flow which lie on curve BC on plane  $c_x, 1/\sigma$  (cf. figure 13). Point B, as before, corresponds to limit constant-property flow  $(p_{0p})_B = 0$ .

Obviously, only one point on this curve can represent real flow, since  $\sigma_{exp}$ , the experimental constant for a turbulent mixing layer, is not a function of the shape of the body and separation area.

There are three possible cases.

Case 1:  $1/\sigma_{exp} < (1/\sigma)_B$  -- the assumed steady flow with quiescent fluid within the separation area does not exist. Flow with a circulation core may exist, but it cannot be calculated without regard for turbulent friction stresses and energy dissipation within the core.

Case 2:  $1/\sigma_{exp} > (1/\sigma)_B$  -- the assumed steady flow with quiescent fluid within the separation area does not satisfy the determination rule and cannot in fact be realized as steady.

Case 3:  $1/\sigma_{exp} = (1/\sigma)_B$  -- the assumed steady flow with quiescent fluid within the separation area exists and, since it satisfies the determination rule, can be realized in reality.

Since  $(1/\sigma)_B$  is a function of body shape, and  $1/\sigma_{exp}$  is constant, the probability that the proposed steady flow pattern with separation area will be observed in experiments with a random body shape is quite low.

Thus, calculation of a turbulent separation area using a pure element -- a turbulent mixing layer -- is correct in those particular cases when the two conditions below are simultaneously satisfied:

$$u_b \approx 0.7, \quad (1/\delta)_B \approx 1/\delta_{exp} \quad (7.1)$$

If condition (7.1) is not fulfilled, flow in a separation area will be unsteady (i.e. it will possess increased pulsation amplitude in the turbulent mixing layer and a frequency characteristic different from that of an isolated (pure) turbulent mixing layer) or will remain steady, but will have a circulation core. In either case, calculation based on the concept of a pure mixing layer is unsuitable.

In view of what has been presented here, it is obvious that the calculating procedure proposed by Korst [16] to describe actual turbulent flows with separation areas is incorrect. This procedure uses the concept of a pure turbulent mixing layer, but, of the three hydrodynamic equations which describe flow, only one -- the equation of preservation of mass -- is satisfied.

Therefore, it is still absolutely necessary to satisfy conditions of type (7.1) to realize the proposed pattern of flow resulting from this complete system of hydrodynamic equations. It is conceivable that the well-known discrepancy between

---

<sup>7</sup> That is, the dissipator's characteristic is close to that of an ideal dissipator.

calculated data obtained using Korst's method and data from systematic French [17] and English [18] experiments results because the flow pattern assumed in the calculation procedure cannot be realized in reality due to the fact that conditions of type (7.1) cannot be fulfilled. Note also that the failure /19 to satisfy the momentum equation in Korst's procedure leads to a paradoxical, but clearly unjustified, conclusion that we do not need to know of the value of the experimental constant  $\sigma_{exp}$  to calculate base pressure if there is turbulent flow in a separation area and no mass exchange between the separation area and the body.

2. Laminar flow in a separation area with unfixed flow separation point. Experiments on this important class show that flow in a laminar separation area is steady and has a circulation core over a wide range of R numbers up to about  $10^6$  if  $M > 1$ .

This flow has two regions for which calculations are done entirely differently: region I before the separation area to the flow separation point can be calculated (as is done in many studies using variations of integral ratio method) regardless of pressure within the separation area or taper; region II between the flow separation point and attachment, containing a circulation core, whose parameters are a function of the intensity of the descending jump or of taper. Calculating viscous flow in region II at high R numbers is a difficult problem whose solution requires effective methods which account for all the features of complex flow with sufficient accuracy, but which have not yet been found. We might expect that, as difficulties in numerical calculation of steady flow are overcome, we will be confronted by the problem of determining a single, practicable solution which must be reliable.

In view of what has been presented here, it is conceivable that determination should also be made in terms of the configuration of flow in the nonviscous vortical attachment

region. To adapt the determination rule in this case, flow in a certain finite attachment region must be calculated as vortical and nonviscous.

## REFERENCES

1. Lessen, M., On the stability of the free laminar boundary layer between parallel streams, NACA, Rep. 979, 1949.
2. Lock, R. C. The velocity distribution in the laminar boundary layer between parallel streams, Quart. J. Mech. and Appl. Math., 1951, vol. 4, No. 1, p. 42
3. Efros, D. A. Hydrodynamic theory of flat parallel cavitation flows, Dokl. AN SSSR, 1946, vol. 51, No. 4.
4. Gurevich, M. I., Teoriya struy ideal'noy zhidkosti [A Theory of Jets of an Ideal Fluid], Moscow, Fizmatgiz, 1961.
5. Batchelor, G. K., On steady laminar flow with closed streamlines at large Reynolds number, J. Fluid Mech. 1956, vol. 1, pt. 2.
6. Batchelor, G. K., A proposal concerning laminar wakes behind bluff bodies at large R numbers, J. Fluid Mech., 1956, vol. 4, pt. 4, p. 386.
7. Lavrent'yev, M. A., Variatsionnyy metod v krayevykh zadachakh dlya sistem uravneniy ellipticheskogo tipa [Variational Method in Extremum Problems for Systems of Elliptical Type Equations], Moscow, Academy of Sciences of the USSR Press, 1962.
8. Nikol'skiy, A. A., On flat vortical movements of gases, in Nekotoryye tochnyye resheniya uravneniy prostranstvennykh techeniy gasa [Some Precise Solution to Equations of Three-dimensional Gas Flow], Tr. TsAGI, 1949.
9. Ablow, C. M., Hayes, W. D., Perturbation of free surface flows. Technical Report No. 1, Office of Naval Research, No. 7 onr-35807, Graduate Division of Applied Mathematics, Brown University, 1951.
10. Fox, J. L., Morgan, G. M., On the stability of some flows of an ideal fluid with free surfaces, Quart. Appl. Math. 1954, vol. 11, No. 4, pp. 439-456.
11. Thom, A., Flow past circular cylinders at low speeds, Proc. Roy. Soc., 1933, A 141.
12. Grove, A. S., Shair, F. H., Petersen, E. E., Acrivos, A., An experimental investigation of steady separated flow past a circular cylinder, J. Fluid Mech., 1964, vol. 19, pt. 1, p. 60.

13. Sedov, L. I., Ploskiye zadachi gidrodinamiki i aerodinamiki [Flat problems in hydrodynamics and aerodynamics], Ed. 2, Moscow, "Nauka," 1966.
14. Chapman, D. R., Kuehn, D. M., Larson, H. K., Investigation of separated flows in supersonic and subsonic streams with emphasis on the effect of transition, NACA Rep. 1356, 1958.
15. Roshko, A., On the wake and drag of bluff bodies, J. Aeronaut. Sci., 1955, vol. 22, No. 2, p. 124.
16. Korst, H. H., A theory for base pressures in transonic and supersonic flow, J. Appl. Mech., 1956, vol. 23, No. 4, pp. 593-600.
17. Carrier, P., Recent studies by ONERA on problems of attachment, 7th Fluid Dynamic Symposium, Jurata, Poland, 1965.
18. Nash, J. F., An analysis of two-dimensional turbulent base flow including the effect of the approaching boundary layer, ARC RM, 1963, No. 3344.

END

DATE

FILMED

JUN 27 1985

LANGLEY RESEARCH CENTER



3 1176 00188 6671

